Unified description of nondiffracting *X* and *Y* waves

J. Salo,[1] J. Fagerholm,[2] A. T. Friberg,[3] and M. M. Salomaa[1]
[1]*Materials Physics Laboratory, Helsinki University of Technology, P.O. Box 2200 (Technical Physics), FIN-02015 HUT, Finland*
[2]*Center for Scientific Computing (CSC), P.O. Box 405, FIN-02101 Espoo, Finland*
[3]*Department of Physics-Optics, Royal Institute of Technology, SE-10044 Stockholm, Sweden*
(Received 3 January 2000)

A unified spectral and temporal representation is introduced for nondiffracting waves. We consider a set of elementary broadband *X* waves that spans the commonly considered nondiffracting wave solutions. These basis *X* waves have a simple spectral representation that leads to expressions in closed algebraic form or, alternatively, in terms of hypergeometric functions. The span of the *X* waves is also closed with respect to all spatial and temporal derivatives and, consequently, they can be used to compose different types of waves with complex spectral and spatial properties. The unified description of Bessel-based nondiffracting waves is further extended to include singular Neumann and Hankel waves, or *Y* waves. We also discuss connections between the different known nondiffracting wave solutions, and their relations to the present unified approach.

PACS number(s): 43.20.+g, 42.25.Bs, 46.40.Cd, 62.30.+d

I. INTRODUCTION

Nondiffracting waves have attracted intense attention after Durnin *et al.* [1] first reported the generation of an optical diffraction-free beam, also referred to as a Bessel beam, in 1987. Although the monochromatic solution had originally been presented by Stratton [2]—as early as 1941—the polychromatic waves remained relatively ignored until Lu and Greenleaf [3] first introduced nondiffracting acoustic pulses, and subsequently presented a theoretical derivation of nondiffracting *X* waves [4].

Several different approaches to nondiffracting waves have been proposed. Lu and Greenleaf themselves also suggested another scheme in which one transforms an ordinary wave solution in an $(n-1)$-dimensional space into a nondiffracting solution in an n-dimensional space; when applied to wavelet solutions, it was called a wavelet transform [5]. We have discussed nondiffracting waves using the angular spectrum of plane waves, and analyzed new solutions obtained as temporal derivatives of the fundamental *X* wave [6,7]. A temporal, instead of spectral, approach to nondiffracting waves was suggested by Stepanishen and Sun [8,9]. Recently, we re-derived nondiffracting waves using their Fourier representation to generalize *X* waves into anisotropic wave propagation [10].

In the present paper, we obtain a general expression for nondiffracting waves using their Fourier transforms. This leads to the spectral representation of nondiffracting waves, which is here subsequently converted into a temporal representation. We derive an algebraic expression for an important subclass of broadband *X* waves and show that this subclass of wave solutions is closed with respect to all temporal and spatial derivatives. This simplifies in an essential way the description of derivative-based mixed-wave modes, such as the bowtie [11] and array waves [12].

We define nondiffracting waves as such solutions of the wave equation that propagate uniformly—invariant in shape—along a given direction with a fixed velocity v, called the velocity of propagation. Mathematically, the wave is expressed as $\phi(x,y,z;t)=f(x,y,z-vt)$. This leads to polychromatic generalizations of Bessel beams. We also discuss ''extended'' nondiffracting waves that are based on the Neumann or Hankel—instead of Bessel—beams [13,14]. Noting that the cross section of the Hankel waves resembles the capital letter *Y*, we suggest for them the name ''*Y* waves.'' We also analyze the spectral and azimuthal degrees of freedom exhibited by nondiffracting waves.

We explicitly consider an important subclass of nondiffracting waves that we refer to as *X* waves. These are waves with a spectrum of the form $\omega^m e^{-\alpha\omega}$. We have already presented these solutions and analyzed their properties using the angular-spectrum representation [6,7]. Here we represent them in closed algebraic form. The original definition of nondiffracting *X* waves [4] is more general and contains essentially all nondiffracting waves. The X-shaped form of the wave is, however, most pronounced for this subclass of wave solutions, and we refer to the more general class of solutions merely as nondiffracting waves.

Finally, we consider different known nondiffracting wave solutions and discuss connections between the notations in this field. This is to assist further studies on the subject and to help clarify the significance of and interrelations between the many contributions.

II. PHYSICS OF NONDIFFRACTING WAVES

Nondiffracting waves provide propagating beams and pulses that feature good spatial localization—of the order of wavelength—without diffractive effects that would divert similarly localized Gaussian waves. Physically, diffractive spreading of waves is avoided provided that the wave propagates invariant in shape, which is the mathematical premise for the unified formulation of the present paper for nondiffracting waves. Since nondiffracting waves are supposed to propagate in free homogeneous media they may be constructed as linear combinations of plane waves. The condition of uniform propagation requires that all plane-wave components share a common phase velocity in the direction of propagation. Consequently, they remain in phase and the wave possesses an invariant form.

For monochromatic nondiffracting beams, the cross section of the wave is invariant in the axial direction, the z axis, while it features a peaked amplitude maximum in the (x,y) plane. The peak itself can be made as narrow as the wavelength without spreading effects. On the other hand, the requirement of uniform propagation unavoidably leads to a transverse component of the energy flux that is needed to support the main peak of the wave. It is observed in (an infinite number of) relatively strong side lobes and the wave energy decreases only in proportion to r^{-1} far from the axis of propagation. Nevertheless, even finite-aperture approximations of nondiffracting beams show a wavelength-wide focal line of arbitrary length in the axial direction, and energy concentration along this focal line.

The energy propagation within nondiffracting waves is manifestly seen in pulselike X waves; they consist of conical wavefronts that carry the wave energy. The fronts extend a fixed angle (defined by the velocity of the pulse) with the axis of propagation, and the propagating pulse is observed at the crossing of the wavefronts. Thus, the energy of the pulse does not propagate along the axis of propagation, but is provided by the conical wavefronts that carry energy from the outer regions of the aperture. The characteristic structure of nondiffracting waves is revealed in the ''fundamental X wave'' that is illustrated in Fig. 1 and further discussed in Sec. VII.

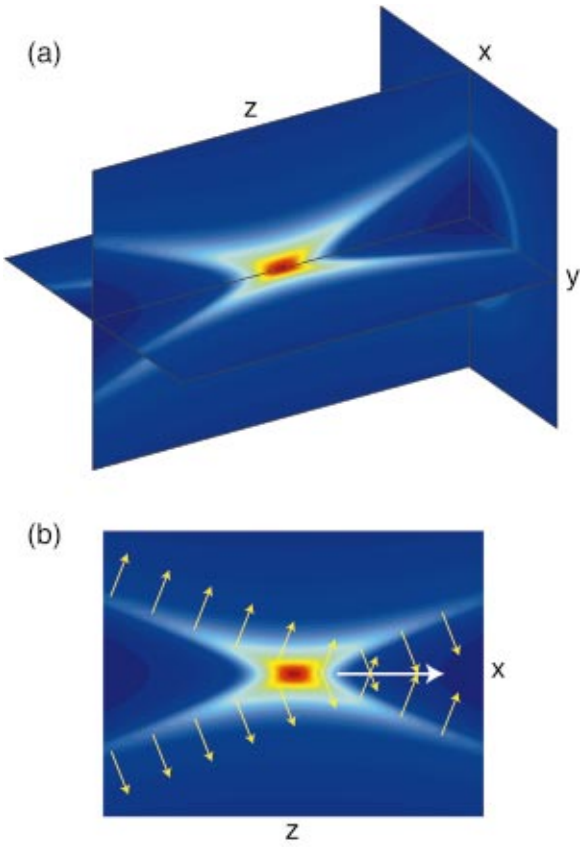

FIG. 1. (Color) Fundamental X wave $\Phi_{0,0}$. (a) Cone of propagation characteristic to all nondiffracting waves. The direction of propagation is along the z axis. The focal spot and the wave pattern appear to propagate with superluminal velocity. (b) The (x,z) cut of the same wave. Small arrows represent the energy flow that coincides with the propagation of the wavefronts while the large arrow indicates the propagation of the entire wave. The focal spot is formed as the superposition of wavefronts. Since the wave is symmetric about the z axis, the wavefronts are conical in three dimensions. For the $n=0$ wave, the energy flux has no azimuthal component and the wavefronts cross on the z axis. For higher azimuthal orders, the flux also possesses an azimuthal component and the wavefronts no longer cross in a single center, which causes the higher-order waves to be so-called ''dark pulse'' waves.

III. UNIFIED FORMULATION

A nondiffracting wave is defined as a solution to the scalar wave equation that propagates uniformly along the z axis with the velocity of propagation v. Such a wave may be expressed as $\phi(x,y,z;t)=f(x,y,z-vt)$, and its Fourier representation is [15]

$$\tilde{\phi}(k_x,k_y,k_z;\omega)=\frac{1}{(2\pi)^2}\int \phi(x,y,z;t) \times e^{-i(k_x x+k_y y+k_z z-\omega t)}d\mathbf{r}dt. \quad (1)$$

Changing the variables of integration into $\eta=z-vt$ and $\theta=z$ leads to

$$\tilde{\phi}(k_x,k_y,k_z;\omega)=\delta(k_z-\omega/v)\frac{\sqrt{2\pi}}{v}\tilde{f}(k_x,k_y,\omega/v), \quad (2)$$

where $\tilde{f}$ is the Fourier transform of f, either of which may be taken arbitrary. However, the Fourier representation of the wave itself proves proportional to $\delta(k_z-\omega/v)$, which is a sufficient condition for the wave to propagate uniformly along the z axis. The wave is also required to satisfy the wave equation, which holds assuming that $k_x^2+k_y^2=k_\perp^2=\omega^2/c^2-k_z^2$, where c is the speed of light (or sound) in the medium and $k_\perp$ is the radial wave number. This is satisfied by construction provided that we choose the representation

$$k_x=\omega(\sin\zeta)(\cos\beta)/c,$$
$$k_y=\omega(\sin\zeta)(\sin\beta)/c, \quad (3)$$
$$k_z=\omega(\cos\zeta)/c.$$

Due to the nondiffraction condition, $k_z=\omega/v$, we deduce that $v=c/\cos\zeta\geqslant c$ (since $v>0$ and thus $0\leqslant\zeta\leqslant\pi/2$). The radial wave number assumes the form

$$k_\perp=\omega(\sin\zeta)/c \quad (4)$$

and β in Eq. (3) is the azimuthal angle in the (k_x,k_y) plane. Above, $\zeta=0$ corresponds to a plane wave, while $\zeta=\pi/2$ would imply a wave independent of z, which formally has an infinite velocity of propagation along z. The parameter ζ is called the axicon angle of the wave, see Ref. [16], and its value is determined by the velocity of propagation [17]. Below, we find that the axicon angle defines a cone of propagation that is characteristic to all nondiffracting waves having equal velocities.

Consequently, the Fourier transform of an arbitrary nondiffracting wave is of the form

$$\tilde{\phi}(\mathbf{k},\omega)=f(\omega,\beta)\,\delta(k_\perp-\omega(\sin\zeta)/c)\,\delta(k_z-\omega(\cos\zeta)/c). \tag{5}$$

The latter delta function, containing k_z, arises from the nondiffraction condition, while both delta functions together ensure that the wave equation be satisfied.

We point out that the above expression [Eq. (5)], is essentially identical to that presented by Donnelly *et al.* [see Ref. [18], Eq. (11)]:

$$\Psi_\gamma(\mathbf{k},\omega)=\Xi(\kappa,\gamma)\,\delta(k_z-\gamma\kappa/\sqrt{1-\gamma^2})\,\delta(\omega-c\kappa/\sqrt{1-\gamma^2}), \tag{6}$$

where κ is the radial wave number and $\gamma\in(-1,1)$ is a free parameter. According to this representation, the velocity of propagation is $v=\omega/k_z=c/\gamma$ whence $\gamma=\cos\zeta$ in our notation.

A. Spectral approach

Since β is limited into the finite interval $[0,2\pi]$, we may express $f(\omega,\beta)$ as the Fourier series

$$f(\omega,\beta)=\sum_{n=-\infty}^{\infty} f_n(\omega)e^{in\beta}. \tag{7}$$

This shows that any nondiffracting wave is a superposition of components with well-defined azimuthal properties, i.e., azimuthal order *n*. Below we show that the azimuthal dependence in real space also shares the same functional form $e^{in\varphi}$. Considering a wave for fixed *n*, we obtain

$$\tilde{\Phi}_n(\mathbf{k},\omega)=e^{in(\beta-\pi/2)}f_n(\omega)\frac{2\pi}{k_\perp}\delta(k_\perp-\omega(\sin\zeta)/c)\times\delta(k_z-\omega(\cos\zeta)/c). \tag{8}$$

The arbitrary function $f_n(\omega)$ is called the spectrum of the nondiffracting wave. The factor $2\pi/k_\perp$ arises from the measure of integration in cylindrical coordinates [19]. We emphasize that all nondiffracting waves (with a common velocity and direction of propagation) in free space can be expressed as a sum of waves of this form. This shows that the original *X* waves [4] are the most general nondiffracting waves, except for being limited to positive frequencies only. The inverse Fourier transform leads to

$$\Phi_n(\mathbf{r},t)=\int_{-\infty}^{\infty} f_n(\omega)\Phi_{J_n}(r,\varphi,z,t;\omega)\,d\omega, \tag{9}$$

which is a spectral generalization of Bessel beams of the form

$$\Phi_{J_n}(r,\varphi,z,t;\omega)=(-1)^{*n}e^{in\varphi}J_{|n|}(\omega r(\sin\zeta)/c)\times e^{i[(\cos\zeta)z/c-t]\omega}, \tag{10}$$

where we introduce the notation

$$(-1)^{*n}=\begin{cases}1, & n\geq 0\\ (-1)^n, & n<0.\end{cases} \tag{11}$$

Although the index *n* in the Bessel function may also assume negative values, the absolute value is chosen for convenience as it will prove simpler below.

Since $v=c/\cos\zeta$ is the velocity of propagation of the wave, all nondiffracting waves are composed of Bessel beams having different frequencies but the same velocity of propagation. Each Bessel wave has the radial wave number $k_\perp=\omega(\sin\zeta)/c$ and the axial wave number $k_z=\omega(\cos\zeta)/c$ in accordance with Eq. (3). The general expression for a nondiffracting wave is given by summing over the azimuthal degrees of freedom *n*. The function $f_n(\omega)$ represents the temporal spectrum of the nondiffracting wave of azimuthal order *n* and it is also sometimes called the transfer function of the system [4]. We point out that general Fourier theory does not constrain the spectrum $f_n(\omega)$ to positive frequencies. If we require, however, that the nondiffracting wave is represented as the real part of a complex analytic function, the spectral function $f_n(\omega)$ must be limited to positive frequencies only. This will be the case for all nondiffracting wave solutions considered in this paper, apart from the impulse-response waves that also contain negative frequencies.

Here we want to compare this result with the original definition of nondiffracting *X* waves by Lu and Greenleaf in Ref. [4], where the expression for *X* waves is written in the form

$$\Phi_{X_n}=e^{in\varphi}\int_0^\infty T(k)J_n(kr\sin\zeta)e^{ik(z\cos\zeta-ct)}dk. \tag{12}$$

Changing the variable of integration into $\omega=ck$ leads to the result given in Eqs. (9) and (10). The only difference is that the interval of integration is no longer limited to positive values, and the index of the Bessel order may also assume negative (integer) values. Although the negative Bessel orders hardly offer anything new for individual wave modes, they do prove necessary in the construction of waves with more complicated azimuthal shapes. Apart from a few technical aspects, the original nondiffracting *X* waves are the most general nondiffracting waves.

B. Impulse approach

Equation (9) represents a nondiffracting wave in terms of its spectral decomposition. Expressing the spectrum $f_n(\omega)$ as a Fourier transform of the impulse function $F_n(t)$,

$$f_n(\omega)=\frac{1}{\sqrt{2\pi}}\int_{-\infty}^{\infty}F_n(t')e^{i\omega t'}dt', \tag{13}$$

the nondiffracting wave may be represented as

$$\Phi_n(\mathbf{r},t)=\int_{-\infty}^{\infty}F_n(t')\Psi_{J_n}(r,\varphi,z,t;t')dt'. \tag{14}$$

Above, the impulse-response wave Ψ_{J_n} is

$$\Psi_{J_n}(r,\varphi,z,t;t') = \frac{1}{\sqrt{2\pi}} \int_{-\infty}^{\infty} \Phi_{J_n}(r,\varphi,z,t;\omega) e^{i\omega t'} d\omega$$

$$= \frac{e^{in\varphi}}{\sqrt{2\pi}} 2 \ \mathrm{Re} \frac{(\sqrt{b^2-\eta^2}+i\eta)^{|n|}}{b^{|n|}\sqrt{b^2-\eta^2}} \qquad (15)$$

for even n and

$$\Psi_{J_n}(r,\varphi,z,t;t') = \frac{(-1)^{*n} e^{in\varphi}}{\sqrt{2\pi}} 2i \ \mathrm{Im} \frac{(\sqrt{b^2-\eta^2}+i\eta)^{|n|}}{b^{|n|}\sqrt{b^2-\eta^2}} \qquad (16)$$

for odd n, where $\eta = t' - [t - (\cos\zeta)z/c]$ and $b = r(\sin\zeta)/c$. We also define complex analytic impulse-response waves $\hat{\Psi}_{J_n}$, which only contain positive frequencies. They are given as

$$\hat{\Psi}_{J_n}(r,\varphi,z,t;t') = \frac{1}{\sqrt{2\pi}} \int_{0}^{\infty} \Phi_{J_n}(r,\varphi,z,t;\omega) e^{i\omega t'} d\omega$$

$$= \frac{(-1)^{*n} e^{in\varphi}}{\sqrt{2\pi}} \frac{(\sqrt{b^2-\eta^2}+i\eta)^{|n|}}{b^{|n|}\sqrt{b^2-\eta^2}}, \qquad (17)$$

and they automatically yield complex analytic nondiffracting waves when inserted into Eq. (14). Note that the complex analytic property is also achieved by using an analytic impulse function $F_n(t)$, in which case the impulse-response wave may either be taken as in Eqs. (15,16) or as in Eq. (17), see Ref. [8].

IV. *X* WAVES

We now turn to consider nondiffracting waves of a specific form. Consider a wave defined by the Fourier representation

$$\tilde{\Phi}_{n,m}(\mathbf{k},\omega) = e^{in(\beta-\pi/2)} H(\omega)\omega^m e^{-\alpha\omega} \frac{2\pi}{k_\perp} \times \delta(k_\perp - \omega(\sin\zeta)/c)\delta(k_z - \omega(\cos\zeta)/c), \quad (18)$$

where $H(\omega)$ is the Heaviside step function that limits the interval of integration to positive frequencies. We also introduce an attenuation factor α which will imply a time and length scale, see below. The wave has two degrees of freedom: an azimuthal order of the wave, $n \in \mathbb{Z}$, and a spectral order, $m \in \mathbb{Z}$, with $m \geq 0$. Being limited to positive frequencies only, the wave has a complex analytic form, and its spectrum is given by $f_n(\omega) = \omega^m e^{-\alpha\omega}$ while the corresponding impulse function is $F_n(t) = (2\pi)^{-1/2} m!(\alpha + it)^{-m-1}$, see Eq. (13).

Waves given by Eq. (18) are single-mode waves with uniquely defined spectral and azimuthal properties. The term *X* wave refers to all linear combinations of waves of this type. This class of nondiffracting waves has the following two properties: (i) all azimuthal degrees of freedom allowed for nondiffracting waves are covered by summing over the index n, and (ii) the spectra of the waves are limited to a specific form, namely, (polynomial of ω)$\times e^{-\alpha\omega}$ that are obtained by linear combinations over different m. The most frequently considered waves are of this form.

TABLE I. Algebraic expressions for *X* waves in some special cases. Here, P_m is a Legendre polynomial and Γ is the gamma function. The main-branch complex square root functions are to be used in these expressions.

$n=m=0$	$\Phi_{0,0}(\mathbf{r},t) = \dfrac{1}{\sqrt{\tau^2+b^2}}$
$n=0$	$\Phi_{0,m}(\mathbf{r},t) = \dfrac{\Gamma(m+1)}{(\tau^2+b^2)^{(m+1)/2}} P_m\left(\dfrac{\tau}{\sqrt{\tau^2+b^2}}\right)$
$m=0$	$\Phi_{n,0}(\mathbf{r},t) = (-1)^{*n} e^{in\varphi} \dfrac{b^{\lvert n\rvert}}{\sqrt{\tau^2+b^2}(\sqrt{\tau^2+b^2}+\tau)^{\lvert n\rvert}}$
$m=\lvert n\rvert$	$\Phi_{\lvert n\rvert,n}(\mathbf{r},t) = (-1)^{*n} e^{in\varphi} \dfrac{(2\lvert n\rvert)!}{\lvert n\rvert! 2^{\lvert n\rvert}} \dfrac{b^{\lvert n\rvert}}{(\tau^2+b^2)^{\lvert n\rvert+1/2}}$

The single-mode wave is now expressed in the form

$$\Phi_{n,m}(\mathbf{r},t) = (-1)^{*n} e^{in\varphi} \int_0^\infty \omega^m J_{|n|}(b\omega) e^{-\tau\omega} d\omega, \quad (19)$$

where $\tau = \alpha - i[(\cos\zeta)z/c - t]$ and $b = r(\sin\zeta)/c$. This can be integrated analytically and the result may be expressed in terms of associated Legendre functions P_μ^ν [see Ref. [20], Eq. 6.621(1)]:

$$\Phi_{n,m}(\mathbf{r},t) = (-1)^{*n} e^{in\varphi} \frac{\Gamma(m+|n|+1)}{(\sqrt{\tau^2+b^2})^{m+1}} P_m^{-|n|}\left(\frac{\tau}{\sqrt{\tau^2+b^2}}\right). \qquad (20)$$

Note that it is necessary that the upper index for the associated Legendre function be negative in this expression since $P_m^n(z) \equiv 0$ for $n > m$. This is the original reason for the introduction of positive Bessel index and the factor $(-1)^{*n}$ in Eq. (10). The parameter m is not limited to integer values only but the wave simplifies essentially for (positive) integer m.

Transforming to the variables $M = \tau^2 + b^2$ and $Q = \tau/\sqrt{\tau^2+b^2}$, the associated Legendre functions can be expressed algebraically (see the Appendix for details), and the wave solution is represented as

$$\Phi_{n,m}(\mathbf{r},t) = (-1)^{*n} e^{in\varphi} \frac{\Gamma(m+|n|+1)}{(\sqrt{M})^{m+1}} \left(\sqrt{\frac{1-Q}{1+Q}}\right)^{|n|} \times \sum_{k=0}^{m} (-1)^k \frac{(m+k)!/(m-k)!}{(|n|+k)!} \frac{(1-Q)^k}{2^k k!}. \qquad (21)$$

Although this expression may appear complicated at first sight, it is easy to evaluate numerically. Furthermore, it simplifies considerably for certain special cases, see Table I. The *X* waves can also be expressed in terms of generalized hypergeometric functions, see Table II. We emphasize that the square roots in Eq. (21) must be taken according to the main

TABLE II. Alternative new representations for X waves using associated Legendre functions and generalized hypergeometric functions. The algebraic expressions require that m assume an integer value while the hypergeometric representations are valid for any real $m \geqslant 0$.

$$\Phi_{n,m}(\mathbf{r},t) = (-1)^{*n} e^{in\varphi} \frac{\Gamma(m+|n|+1)}{(\sqrt{\tau^2+b^2})^{m+1}} P_m^{-|n|}\left(\frac{\tau}{\sqrt{\tau^2+b^2}}\right)$$

$$= (-1)^{*n} e^{in\varphi} \frac{\left(\frac{b}{2\tau}\right)^{|n|} \Gamma(|n|+m+1)}{\tau^{m+1}\Gamma(|n|+1)} {}_2F_1\left(\frac{|n|+m+1}{2}, \frac{|n|+m+2}{2}; |n|+1; -\frac{b^2}{\tau^2}\right)$$

$$= (-1)^{*n} e^{in\varphi} \frac{\left(\frac{b}{2}\right)^{|n|} \Gamma(|n|+m+1)}{\sqrt{(\tau^2+b^2)^{|n|+m+1}}\Gamma(|n|+1)} {}_2F_1\left(\frac{|n|+m+1}{2}, \frac{-m+|n|}{2}; |n|+1; \frac{b^2}{\tau^2+b^2}\right)$$

$$= (-1)^{*n} e^{in\varphi} \frac{\left(\frac{b}{2\tau}\right)^{|n|} \Gamma(|n|+m+1)}{\tau^{m+1}\Gamma(|n|+1)} \left(1+\frac{b^2}{\tau^2}\right)^{1/2-m-1} {}_2F_1\left(\frac{|n|-m}{2}, \frac{|n|-m-1}{2}; |n|+1; -\frac{b^2}{\tau^2}\right).$$

branch with the complex plane cut along the negative real axis. We point out that the associated Legendre functions $P_m^{-|n|}(x)$ are well defined also for $n > m$. However, the function is singular for $x = -1$, but this value of the argument is never achieved for the main branch of the square root in Eq. (20).

A. Normalized time and length scales

Due to the existence of the attenuation factor α, the X waves can be represented in normalized coordinates. The general expression for an X wave is given in Eq. (19):

$$\Phi_{n,m}(\mathbf{r},t) = (-1)^{*n} e^{in\varphi} \int_0^\infty \omega^m J_{|n|}(\omega r(\sin\zeta)/c) \times e^{-\{\alpha - i[(\cos\zeta)z/c - t]\}\omega} d\omega. \quad (22)$$

Changing the variable of integration to $w = \alpha\omega$ yields

$$\Phi_{n,m}(\mathbf{r},t) = \frac{(-1)^{*n}}{\alpha^{m+1}} e^{in\varphi} \int_0^\infty w^m J_{|n|}(wr(\sin\zeta)/(c\alpha)) \times e^{-\{1 - i[(\cos\zeta)z/c - t]/\alpha\}w} dw. \quad (23)$$

Now we introduce normalized coordinates $\hat{r} = r/(c\alpha)$, $\hat{z} = z/(c\alpha)$ and $\hat{t} = t/\alpha$, whereupon the wave in the new coordinates is represented as

$$\Phi_{n,m}(\mathbf{r},t) = \frac{(-1)^{*n}}{\alpha^{m+1}} e^{in\varphi} \int_0^\infty w^m J_{|n|}(w\hat{r}\sin\zeta) \times e^{-[1 - i(\hat{z}\cos\zeta - \hat{t})]w} dw. \quad (24)$$

In this set of coordinates, X waves propagate with the normalized velocity $\hat{v} = 1/\cos\zeta$. We use these scaled coordinates in all the figures.

B. Extended nondiffracting wave solutions

The description of nondiffracting waves employed thus far starts from their Fourier representation. This method is limited to wave solutions that propagate in an infinite free space. If the space is somehow limited, or we allow for external forces, the waves do not fulfill the Fourier space condition given by Eq. (3). An example is provided by spiral waves [13] that have a divergence along the z axis. Sometimes this divergence is of purely mathematical nature with no physical interpretation (Neumann waves, see below), at other times it may be taken as a source or a sink for the wave motion (Hankel waves) [21]. Originally, the spiral nondiffracting waves were taken to be monochromatic, but they can also be generalized to broadband waves.

Since the Neumann functions satisfy exactly the same differential equation as the Bessel functions (apart from the boundary conditions), we may in Eq. (10) replace the Bessel functions with Neumann functions of the same order, or with any linear combinations of them. This leads to Neumann beams

$$\Phi_{Y_n}(r,\varphi,z,t;\omega) = e^{in\varphi}(-1)^{*n} Y_{|n|}(\omega r(\sin\zeta)/c) \times e^{i[(\cos\zeta)z/c - t]\omega}, \quad (25)$$

which represent nondiffracting waves in the volume of space from which the axis of propagation has been excluded. We may also provide a spectral generalization for Neumann beams

$$\Phi_n^Y = \int_{-\infty}^\infty f_n(\omega)\Phi_{Y_n}(r,\varphi,z,t;\omega)\, d\omega, \quad (26)$$

such that we obtain the Neumann X waves for $f(\omega) = \omega^m e^{-\alpha\omega}$ with $m \geqslant n$ [see Ref. [20], Eq. 6.621(2)]

TABLE III. Derivatives of Bessel beams and X waves.

	Φ_{J_n}	$\Phi_{n,m}$
$\frac{\partial}{\partial x}$	$\frac{\omega \sin\zeta}{2c}(\Phi_{J_{n-1}}-\Phi_{J_{n+1}})$	$\frac{\sin\zeta}{2c}(\Phi_{n-1,m+1}-\Phi_{n+1,m+1})$
$\frac{\partial}{\partial y}$	$\frac{i\omega \sin\zeta}{2c}(\Phi_{J_{n-1}}+\Phi_{J_{n+1}})$	$\frac{i \sin\zeta}{2c}(\Phi_{n-1,m+1}+\Phi_{n+1,m+1})$
$\frac{\partial}{\partial r}$	$\frac{\omega \sin\zeta}{2c}(e^{i\varphi}\Phi_{J_{n-1}}-e^{-i\varphi}\Phi_{J_{n+1}})$	$\frac{\sin\zeta}{2c}(e^{i\varphi}\Phi_{n-1,m+1}-e^{-i\varphi}\Phi_{n+1,m+1})$
$\frac{\partial}{\partial \varphi}$	$in\Phi_{J_n}$	$in\Phi_{n,m}$
$\frac{\partial}{\partial z}$	$\frac{i\omega \cos\zeta}{c}\Phi_{J_n}$	$\frac{i \cos\zeta}{c}\Phi_{n,m+1}$
$\frac{\partial}{\partial t}$	$-i\omega\Phi_{J_n}$	$-i\Phi_{n,m+1}$

$$\Phi^{Y}_{n,m}(\mathbf{r},t)=(-1)^{*n}e^{in\varphi}\int_0^\infty \omega^m Y_{|n|}(b\omega)e^{-\tau\omega}d\omega$$

$$=-(-1)^{*n}e^{in\varphi}\frac{2}{\pi}\frac{\Gamma(m+|n|+1)}{(\sqrt{\tau^2+b^2})^{m+1}}$$

$$\times Q_m^{-|n|}\left(\frac{\tau}{\sqrt{\tau^2+b^2}}\right). \tag{27}$$

The associated Legendre functions of the second kind, $Q^{\nu}_{\mu}(x)$, diverge for $x=1$ and the wave is undefined for $b=r=0$, i.e., along the axis of propagation. This integral converges (at $\omega\to 0$) only for $m\geqslant n$ while the opposite circumstance would lead to a non-integrable singularity at zero frequency.

Both the Bessel-type waves and the Neumann-type waves represent ''standing wave'' solutions that propagate energy towards the z axis and away from it with equal energy flux (to be compared with the sine and cosine waves that are superpositions of waves propagating to the left and right). We may also consider their complex superpositions, i.e., Hankel-type waves that propagate energy either towards the z axis or away from it. They represent ''source'' and ''sink'' fields whose energy is not conserved but is created (or annihilated) on the axis of propagation. Using the Hankel functions $H_n^{(1,2)}(x)=J_n(x)\pm iY_n(x)$ [22], we obtain spiral nondiffracting beams (Hankel beams)

$$\Phi^{(1,2)}_{H_n}(r,\varphi,z,t;\omega)=e^{in\varphi}(-1)^{*n}H^{(1,2)}_{|n|}(\omega r(\sin\zeta)/c)$$

$$\times e^{i[(\cos\zeta)z/c-t]\omega}. \tag{28}$$

Nondiffracting Hankel waves are similarly obtained by summing Bessel- and Neumann-based X waves

$$\Phi^{H^{(1,2)}}_{n,m}=\Phi_{n,m}\pm i\Phi^{Y}_{n,m}. \tag{29}$$

Note that the cross section of the Hankel waves only contains a half-cone. Therefore, we introduce for them the name Y wave (see Fig. 7 below and the discussion in Sec. VII).

V. DERIVATIVES OF NONDIFFRACTING WAVES

The Fourier formulation readily yields all temporal and spatial derivatives of nondiffracting waves. Using the Fourier representation [Eq. (8)] and the fact that $k_x=k_\perp\cos\beta=[(\omega\sin\zeta)/(2c)](e^{i\beta}+e^{-i\beta})$, we find

$$\mathcal{F}\left[\frac{\partial\Phi_n}{\partial x}\right]=ik_x\tilde{\Phi}_n=\frac{\sin\zeta}{2c}(\omega\tilde{\Phi}_{n-1}-\omega\tilde{\Phi}_{n+1}). \tag{30}$$

Similarly, the partial derivative with respect to y is given by

$$\mathcal{F}\left[\frac{\partial\Phi_n}{\partial y}\right]=ik_y\tilde{\Phi}_n=\frac{i\sin\zeta}{2c}(\omega\tilde{\Phi}_{n-1}+\omega\tilde{\Phi}_{n+1}). \tag{31}$$

The necessity of introducing nondiffracting waves for negative Bessel orders becomes obvious with spatial derivatives: positive Bessel orders do not span all the spatial degrees of freedom and, especially, they do not cover the derivative waves. The last two derivatives, i.e., the spatial z derivative and the temporal t derivative, are readily obtained from the Fourier representation, and are given by

$$\mathcal{F}\left[\frac{\partial\Phi_n}{\partial z}\right]=i\frac{\cos\zeta}{c}\omega\tilde{\Phi}_n \tag{32}$$

and

$$\mathcal{F}\left[\frac{\partial\Phi_n}{\partial t}\right]=-i\omega\tilde{\Phi}_n. \tag{33}$$

Since Bessel beams are monochromatic nondiffracting waves and the X waves have the simple $\omega^m e^{-\alpha\omega}$ spectrum, their derivatives are readily obtained from the previous expressions, and they are given in Table III. In Table III, we have also included the derivatives with respect to cylindrical coordinates. We conclude that all derivatives of the Bessel beams and the X waves can be expressed in terms of Bessel beams and X waves, respectively. Therefore, both subclasses of nondiffracting waves are closed with respect to all derivatives.

As already emphasized by Lu [11,12], the derivatives of nondiffracting waves can be used to generate new wave solutions with specified azimuthal properties. We shall briefly

consider bowtie and array wave techniques, both of which employ spatial derivatives. In the bowtie waves the energy propagates primarily near the (y,z) plane, leading to a relatively narrow wave in the x direction, while the array waves have several focal spots in the shape of an array, instead of a single focal center. Both techniques start with single-mode waves (usually $n=0$) and, via partial differentiation, lead to new solutions. They are defined as follows:

$$\Phi_n^{B(q)} = \frac{\partial^q}{\partial y^q}\Phi_n , \tag{34}$$

$$\Phi_n^{A(q)} = \frac{\partial^{2q}}{\partial x^q \partial y^q}\Phi_n ,$$

where the superscripts B and A refer to the bowtie and array type waves, respectively; q is the order of the bowtie or array wave, and n is the azimuthal order of the nondiffracting wave used to generate the new waves.

From here on, we limit our discussion to the bowtie and array waves generated by Bessel beams and X waves. Recalling that the derivatives of these only differ owing to the fact that each derivative introduces a factor of ω for the Bessel beams and raises the spectral index m by 1 for the X waves, we choose to consider only X waves explicitly in what follows.

Consider an X wave of orders n and m. It generates a family of bowtie waves

$$\tilde{\Phi}_{n,m}^{B(q)} = (ik_y)^q \tilde{\Phi}_{n,m} = i^q \left(\frac{\omega \sin\zeta}{2ic}\right)^q (e^{i\beta} - e^{-i\beta})^q \tilde{\Phi}_{n,m}$$

$$= \left(\frac{i \sin\zeta}{2c}\right)^q \sum_{p=0}^{q} \binom{q}{p} \tilde{\Phi}_{n-q+2p,m+q} , \tag{35}$$

whence

$$\Phi_{n,m}^{B(q)} = \left(\frac{i \sin\zeta}{2c}\right)^q \sum_{p=0}^{q} \binom{q}{p} \Phi_{n-q+2p,m+q} . \tag{36}$$

Similarly, we obtain bowtie waves generated by Bessel beams:

$$\Phi_{J_n}^{B(q)} = \left(\frac{i\omega \sin\zeta}{2c}\right)^q \sum_{p=0}^{q} \binom{q}{p} \Phi_{J_{n-q+2p}} . \tag{37}$$

Array waves generated by an X wave are in turn given by

$$\tilde{\Phi}_{n,m}^{A(q)} = (ik_x)^q (ik_y)^q \tilde{\Phi}_{n,m}$$

$$= i^q \left(\frac{\sin\zeta}{2c}\right)^{2q} \sum_{p=0}^{q} \binom{q}{p} (-1)^p \tilde{\Phi}_{n-2q+4p,m+2q} , \tag{38}$$

whence

$$\Phi_{n,m}^{A(q)} = i^q \left(\frac{\sin\zeta}{2c}\right)^{2q} \sum_{p=0}^{q} \binom{q}{p} (-1)^p \Phi_{n-2q+4p,m+2q} \tag{39}$$

and

$$\Phi_{J_n}^{A(q)} = i^q \left(\frac{\omega \sin\zeta}{2c}\right)^{2q} \sum_{p=0}^{q} \binom{q}{p} (-1)^p \Phi_{J_{n-2q+4p}} . \tag{40}$$

Since the analytical solutions are known both for Φ_{J_n} and $\Phi_{n,m}$, all the bowtie and array waves are also obtained in closed form. This again emphasizes the completeness of the classes of Bessel beams and X waves.

VI. RESULTS ON NONDIFFRACTING WAVES

Several nondiffracting wave solutions and methods for their generation have been reported after the original introduction of the Bessel beam [1]. In this section, we discuss how the different solutions are related to our unified description of the nondiffracting waves presented above, and applications of the unified formalism. (See Table IV.)

A. Variety of different approaches

The Fourier representation of nondiffracting waves, which has also been employed by Donnelly *et al.* in Ref. [18], naturally leads to the polychromatic generalizations of Bessel beams and, thus, to all ordinary nondiffracting waves [23]. This procedure is essentially identical to the angular spectrum representation [6], since the latter is chosen to be limited to ordinary nondiffracting waves [24]. Piestun and Shamir also employed a Fourier-based method to derive ''generalized propagation-invariant wave fields'' [25], which in the special case of uniform propagation reduce into monochromatic nondiffracting waves, i.e., Bessel beams. However, Fourier-based methods are not the only way to derive nondiffracting wave solutions. A cylindrical representation of the wave equation was originally employed by Lu and Greenleaf [4] and it leads, together with a suitable ansatz, to the general expression for Bessel-based nondiffracting waves.

There is also a mathematically interesting algorithm of converting an $(n-1)$-dimensional ordinary wave solution into an n-dimensional nondiffracting wave solution [5,7]. This is possible since the degrees of freedom of the former solution coincide with those of the latter. Therefore, there is a one-to-one mapping between ordinary two-dimensional (2D) waves and nondiffracting 3D waves. In the Fourier representation, this is apparent since the 2D wave satisfies $k_x^2 + k_y^2 = \omega^2/c^2$ whereas the 3D wave obeys $k_x^2 + k_y^2 = \omega^2/c^2 - k_z^2 = (1/c^2 - 1/v^2)\omega^2$. Applied to the two-dimensional wavelet solution, this yields a three-dimensional nondiffracting wave that corresponds to the X wave $\Phi_{0,2}$. The impulse-response approach [8,9] is readily obtained from the monochromatic Bessel beams via temporal Fourier transformation.

However, it was noticed already by Stratton [2] that the cylindrical wave equation is satisfied by all circular cylinder functions, that is, also by Neumann and Hankel functions, but not along the axis of propagation. It was pointed out by Chávez-Cerda *et al.* [13] that the monochromatic Bessel

TABLE IV. Different nondiffracting wave solutions.

Authors	Spectrum	Comments	Refs.
Chávez-Cerda and co-workers	monochr.	Hankel waves, Sommerfeld radiation condition, and interference of nondiffracting waves	[13,55] [14]
Donnelly, Power, Templemen, and Whalen	$\omega e^{-\alpha\omega}$	Simulation results	[18]
Durnin, Miceli, Jr., and Eberly	monochr.	The original J_0 beam	[1]
Erdélyi *et al.*	monochr.	Microlithography, Fabry-Perot interferometer	[32]
Fagerholm and co-workers	$\omega^m e^{-\alpha\omega}$	Angular spectrum representation, 2D & 3D nondiffracting waves	[6,7]
Hsu, Margetan, and Thompson	monochr.	Planar ultrasonic transducer	[27]
Koike, Yamada, and Nakamura	monochr., pulse	Conical ultrasonic transducer	[26]
Laycock and Webster	monochr.	Optical and microwave applications	[28]
Lu and Greenleaf	$\sin(\omega_0 t)e^{-t^2/t_0^2}$	The original X wave	[3]
Lu and Greenleaf	positive	X waves	[4,43]
Lu, Xu, and Greenleaf	$\omega^2 e^{-\alpha\omega}$	Wavelet transform	[5]
Lu	general	Bowtie and array waves	[11,12]
Lu	monochr.	Design of nondiffracting waves	[35]
Piestun and Shamir	monochr.	Generalized propagation-invariant waves	[25]
Ruschin and Leizer	monochr.	Evanescent Bessel waves	[53]
Saari and Sõnajalg	Gaussian	Optical X waves	[31]
Stepanishen and Sun	general	Impulse-response approach	[8,9]
Stratton	monochr.	Theoretical origin of Bessel waves	[2]

beam itself should not be considered as an elementary solution, but rather as the superposition of two counterpropagating Hankel waves. This is due to the fact that the Bessel beams and their polychromatic generalizations do not satisfy the Sommerfeld radiation condition and, correspondingly, they involve an energy flux emanating from infinity [14]. Physically, a finite aperture will automatically exclude this effect but, nevertheless, the Hankel-type solutions reappear locally with conical transducers [26] that generate only the ''approaching part'' of the cone of propagation (see Figs. 1 and 8). The approaching part of the cone first locally corresponds to the Hankel solution $H^{(2)}$ and subsequently transforms into the Bessel-type solution. Finally, the wave assumes the form of the Hankel $H^{(1)}$ solution which spreads outward from the axis of propagation. A planar transducer with a finite aperture [27,28] may be used to produce both a Bessel-shaped wave that eventually transforms into the Hankel wave $H^{(1)}$, and a second Hankel wave that first obtains the form of a Bessel wave and only then diverts as a first Hankel wave. In the original experiment of Durnin *et al.* [1], the Bessel wave was formed, while both holograms (diffractive elements) [29] and axicons [30] have both been employed to form nondiffracting waves of the Hankel type.

Although mathematically the spectrum of nondiffracting waves may be chosen arbitrarily, the physical systems involved may set limitations on the spectrum. As pointed out by Saari and Sõnajalg [31], a nearly Gaussian spectrum $f(\omega)=\sqrt{\omega}\exp[-\alpha^2(\omega-\omega_0)^2/2]$ should be chosen for optical nondiffracting waves generated by laser devices. This particular form is, in a sense, even more suitable than an ordinary Gaussian spectrum since it tends to zero continuously at low frequencies. Furthermore, the spectrum is limited to positive frequencies only, resulting in a complex analytic signal. The $n=0$ order wave itself is then given by

$$\Phi_n(\mathbf{r},t)\propto\sqrt{1+i\frac{cz\cos\zeta-t}{\omega_0\alpha^2}}\,e^{-[r^2\sin^2\zeta+(z\cos\zeta-ct)^2]/(2c^2\alpha^2)}\times J_0\left[\left(1+i\frac{cz\cos\zeta-t}{\omega_0\alpha^2}\right)r\omega_0(\sin\zeta)/c\right]\times e^{i\omega_0[z(\cos\zeta)/c-t]}, \tag{41}$$

which is approximate but sufficiently accurate for any pulse bandwidth achievable in optics.

B. Applications of the unified theory

In this paper, we have presented a systematic study of nondiffracting wave solutions, with an emphasis on different spatial and dynamic degrees of freedom compatible with the nondiffraction requirement. By now, a large variety of applications has been proposed for nondiffracting waves and, in particular, for the zero-order Bessel beam as it offers a long focal line, that makes it useful in lithography [32] and imaging applications of wavelength accuracy [33]. Nonetheless, higher-order Bessel beams and beams of more complicated spatial structures have also attracted increasing attention. Since they lack the circular symmetry of the J_0 Bessel beam, two-dimensional acoustic array transducers have been employed in their excitation [34]. Up to the discretization accuracy, such transducers may be optimized to excite arbitrary nondiffracting beams [35]. In optical systems, complicated nondiffracting beams are obtained from (Gaussian) laser beams with diffractive elements [36] or by using the polarization properties of light [37]. In particular, diffractive elements may be employed to produce complicated wave patterns and, for instance, rotating helical waves by superposing Bessel beams having different velocities of propagation [38].

Recently, an interesting application for high-order ''dark'' beams has been suggested in confining cold atoms into an optical atom guide formed by the dark center of the beam [39]. Millimeter-wave diffractive elements may also prove useful in the generation of radio-frequency nondiffracting beams [40].

Nondiffracting waves also encompass periodic beam arrays [41], which, in our approach, resemble array beams of infinite order. Beam arrays consist of a two-dimensional lattice of ''beams'' and they contain only a finite number of plane-wave components. Formally, they may be expressed as a sum of Bessel beams but they are more conveniently analyzed as convolutions of Bessel beams (usually of rather low order) and distributions of lattice points. Beam arrays are suggested to be useful for free-space optical interconnects [42].

As demonstrated in the first experiment [43], nondiffracting pulses have potential in dynamic imaging applications. The time dependence of nondiffracting pulses also requires dynamic apertures that can be controlled both spatially and temporally. In acoustic applications, this may be realized either with circular-symmetric annular transducers [44] (for the $n=0$ pulses), or with real two-dimensional transducer arrays [45] that allow more complicated spatial structures. A truly dynamic transducer allows us to choose the spectral contents of the waves freely, leading to a large variety of different forms of acoustic bullets [8,9]. While dynamic multielement antenna arrays could also be used to send radio-frequency nondiffracting pulses [46], optical *X* waves [47] are obtained as nondiffracting beams with very short lifetime between the ignition and extinction of the beam. In addition to imaging applications, electromagnetic *X* waves have recently been suggested, e.g., for radio communication [48].

VII. PHYSICAL PROPERTIES OF NONDIFFRACTING WAVES

Heretofore, we have considered the purely mathematical construction of nondiffracting waves. Now we turn to describe the physical properties of the various specific nondiffracting wave solutions presented above.

Prior to considering more complicated nondiffracting wave solutions, we briefly discuss the fundamental *X* wave $\Phi_{0,0}$, that illustrates the general conical shape characteristic to all nondiffracting waves. The wave equation together with the nondiffraction condition fixes the ratio of the radial and axial wave vectors according to $k_\perp=(\omega/c)\sin\zeta$ and $k_z=(\omega/c)\cos\zeta$. Since the wave equation under consideration is isotropic and nondispersive, the velocity of the energy flow is necessarily equal to the phase velocity c.

Figure 1 represents the fundamental *X* wave and the energy flow within the wave. Although the structure of the spot itself differs for more complicated waves, the asymptotic conical shape remains common to all broadband waves.

A. Impulse-response waves

Impulse-response waves [Eq. (14)] are nondiffracting waves that correspond to a unit impulse in the time domain. The actual physical waves are obtained as a convolution of the impulse functions and the impulse response waves, but the mere impulse-response waves may be interpreted as the limiting case of a broadband nondiffracting wave having a very low attenuation at high frequencies. As such, they should be considered archetypes of nondiffractive waves rather than their physical realizations.

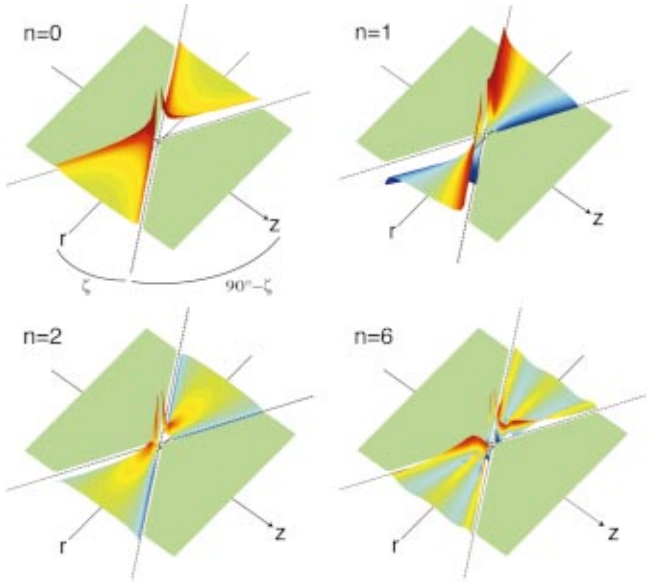

FIG. 2. (Color) Impulse-response waves for orders $n=0$, 1, 2, and 6. The waves of orders 0, 2, and 6 are purely real while the wave of order 1 is purely imaginary. The amplitudes of the waves diverge for $r\sin\zeta=|z|\cos\zeta$. The cone of propagation is obtained by rotating the wave about the z axis. The two disjoint insides of the cone contain no wave motion, which is bound to the outside of the cone.

In Fig. 2, we illustrate four impulse-response waves; those of orders $n=0$, 1, 2, and 6. The impulse waves illustrate the *X*-wave nature of all the nondiffracting waves: the energy of the wave is concentrated on the cone of propagation whose axis coincides with the propagation direction. The opening angle of this cone is defined by the axicon angle parameter and it is $90°-\zeta$ (see Fig. 2). The cross section of the cone with the (x,z) plane has the shape of the letter *X*. The impulse-response waves also have the special property that the wave is strictly bound to the outside of the cones, i.e., for $r\sin\zeta>|z|\cos\zeta$, while the volume inside the cones is free of wave motion. The energy of the wave is concentrated into the vicinity of the cones where the amplitudes of the impulse-response waves diverge. This divergence is, however, integrable and it vanishes in the convolution with the impulse function of the physical wave.

B. *X* waves

The set of *X* waves has many physically and mathematically appealing properties that justify their treatment as one of the most important special cases of nondiffracting waves. In this connection we want to emphasize that there actually is an infinite number of sets of *X* waves: the defining expression, given by Eq. (18), depends on two parameters. The axicon angle is the angle between the k_z axis in the Fourier space and the direction of the actual wave vectors (cf. Ref. [6], Fig. 2). This parameter is used to define the scaling of k_z with frequency; hence, it defines the velocity of propagation

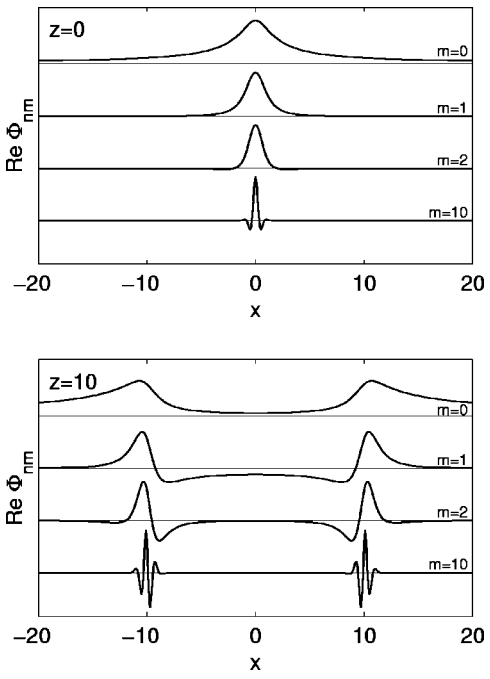

FIG. 3. Above: Waist ($z=0$) of X waves for the orders $m=0$, $m=1$, $m=2$, and $m=10$. The azimuthal order is $n=0$ and the axicon angle is $\zeta=45°$ for all. Below: Approaching forms ($z=10$) of these waves. The X waves become increasingly localized for large m since the spectrum of the wave, $\omega^m e^{-\alpha\omega}$, becomes concentrated for high frequencies. The zero-order wave ($m=0$) is strongly delocalized which is due to the diverging spectrum for zero frequency [the $1/k_\perp$ factor in Eq. (18)]. Oscillations of the higher spectral modes can also be observed. The graphs display the real parts of the waves. Each wave has been scaled individually.

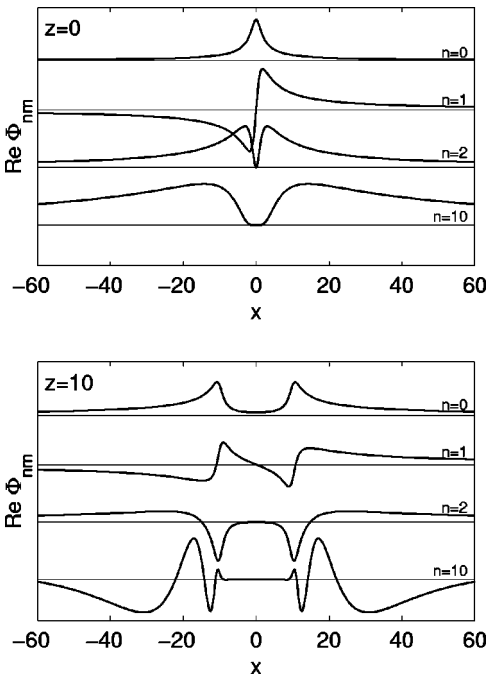

FIG. 4. Above: Waist ($z=0$) for X waves of the azimuthal orders $n=0$, $n=1$, $n=2$, and $n=10$. The spectral order is $m=0$ and the axicon angle is $\zeta=45°$ for all. Below: Approaching forms ($z=10$) of these same waves. While the increasing spectral order m leads to more localized waves, the growing azimuthal order n, in turn, makes them less localized. For high azimuthal orders, the X wave also concentrates to the outside of the cone of energy propagation. The radius of the cone at $z=10$ is $R=10$. The wave for $n=1$ has odd parity with respect to x, owing to the factor $e^{in\varphi}$.

$v=\omega/k_z=c/\cos\zeta$. The other parameter is the attenuation factor α that damps the high-frequency components. The X waves defined through different choices for these parameters are, however, mutually reducible to each other. Therefore, we consider only one set of X waves, with fixed but arbitrary values for these parameters. We assume the values of the parameters to be $\zeta\in(0,\pi/2)$ and $\alpha\in(0,\infty)$.

The existence of the attenuation factor α is quite useful in defining an effective frequency scale since high frequencies are damped according to $\exp[-\alpha\omega]$, whence the ''frequency unit'' is $1/\alpha$. Single-mode X waves $\Phi_{n,m}$ also have an effective frequency. Although the spectrum of X waves has a nonvanishing value for all positive frequencies, it reaches its maximal value at $\omega_{\max}=m/\alpha$. The fundamental X wave $\Phi_{n,0}$ displays a spectral maximum at zero frequency, which is hardly physical in optics. The spectral maximum of higher modes may be varied using different values for the attenuation factor α and also the spectral order, m. The effect of the spectral order m can be seen in Fig. 3. Since the dominating frequencies for the higher spectral modes are also higher, the X waves become increasingly localized for increasing m. This is due to the fact that the spatial Fourier components (k_z and $k_\perp$) scale with frequency and, thus, also obtain large values. This allows for better spatial localization. In this respect, the fundamental mode $\Phi_{n,0}$ proves somewhat complicated. Since the Fourier representation of the X waves [Eq. (18)] also contains the factor $1/k_\perp$, the Fourier transform of the wave diverges for small frequencies. This makes the fundamental mode least localized [49], as can be seen in Fig. 3. The increasing spectral order also causes the waves to be increasingly oscillatory near the axis of propagation.

Also, the azimuthal order of the wave affects the degree of localization of the wave. Since the Bessel beams of orders $|n|\geqslant 1$ exhibit a zero on the z axis, the corresponding X waves also display a zero on the z axis. Hence, the maxima of the waves are located at some finite distance from the axis of propagation. The larger the azimuthal order $|n|$, the farther the maximum is from the axis of propagation. Although the order n has no effect on how fast the wave decays for large r, the halfwidth of the wave increases for high azimuthal orders, see Fig. 4. The azimuthal order also delocalizes the wave in the direction of propagation. Although the wave remains outside the cone of propagation, it no longer is concentrated in the vicinity of the cone. The wave also becomes oscillatory outside the cone (see Fig. 5).

C. Mixed-wave modes

According to Eqs. (7) and (9), the most general expression for nondiffracting waves may be written as

$$\Phi(\mathbf{r},t)=\sum_{n=-\infty}^{\infty}\int_{-\infty}^{\infty}f_n(\omega)\Phi_{J_n}(r,\varphi,z,t;\omega)d\omega, \qquad (42)$$

where the wave is divided into components of different azimuthal orders. In the general case, the spectra of the modes are mutually independent. We point out that the spectral

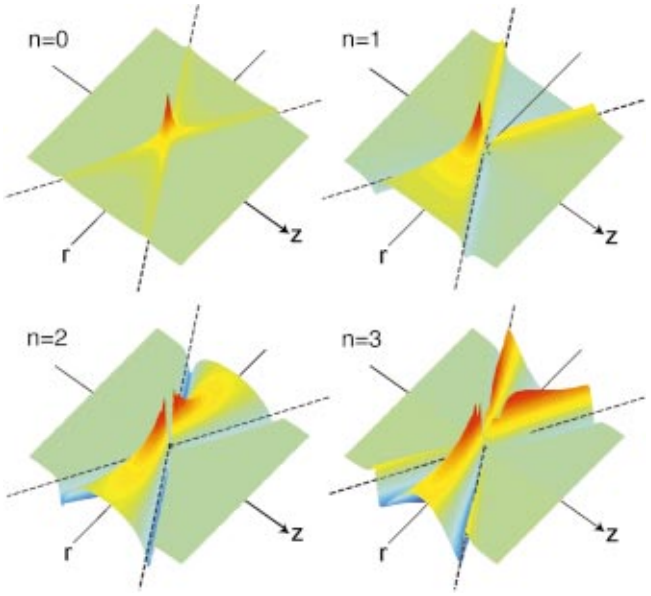

FIG. 5. (Color) *X* waves of different azimuthal orders, *n*. For higher orders, the wave is no longer localized near the cone of propagation but spreads outside the cone. Although the wave decays for large *r*, the waist of the central pulse is strongly broadened (see also Fig. 4).

functions f_n also serve as weight functions for the different modes, although these weights are sometimes frequency dependent. If the spectra are the same for each mode, up to constant factors, they may be referred to as the weights of each mode. In this case, the wave is represented as

$$\tilde{\Phi} = \sum_{n=-\infty}^{\infty} c_n \int_{-\infty}^{\infty} f(\omega)\Phi_{J_n}(r,\varphi,z,t;\omega)\,d\omega, \qquad (43)$$

where the spectrum of the whole wave is merely $f(\omega)$ while the (complex) weights c_n define the contribution of each mode. Usually, the weights tend to zero for high indices, but this does not always hold [50]. Often, most of the weights are zero, either for a practical reason (a finite, instead of an infinite sum), or a theoretical reason (only a finite number of terms appears in the derivative waves).

The simplest example of a mixed-wave mode is obtained as the superposition of two waves with $n_2 = -n_1$. Since, apart from the factor $(-1)^{*n}e^{in\varphi}$, the wave is independent of the sign of the azimuthal order, the resultant wave has an azimuthal form given by $\sin(n\varphi)$ or $\cos(n\varphi)$. This transforms the ''rotating'' $e^{in\varphi}$-shaped wave into a ''nonrotating'' sin- or cos-shaped wave [51]. However, the ''rotating'' wave is not actually rotating since the physical wave still propagates uniformly according to $\phi(x,y,z-vt)$. More complicated mixed-wave modes are obtained from spatial derivatives (see Table III), and from different techniques based on derivatives, like the bowtie waves [11] and array waves [12]. Although the grid and layered array beams may technically be obtained by summing an infinite number of different Bessel beams, they are actually merely superpositions of two or four plane waves. There also exist methods to directly design nondiffracting waves where the weights of the different modes are optimized to form a wave of designed shape [35]. See Fig. 6 for the bowtie and array waves.

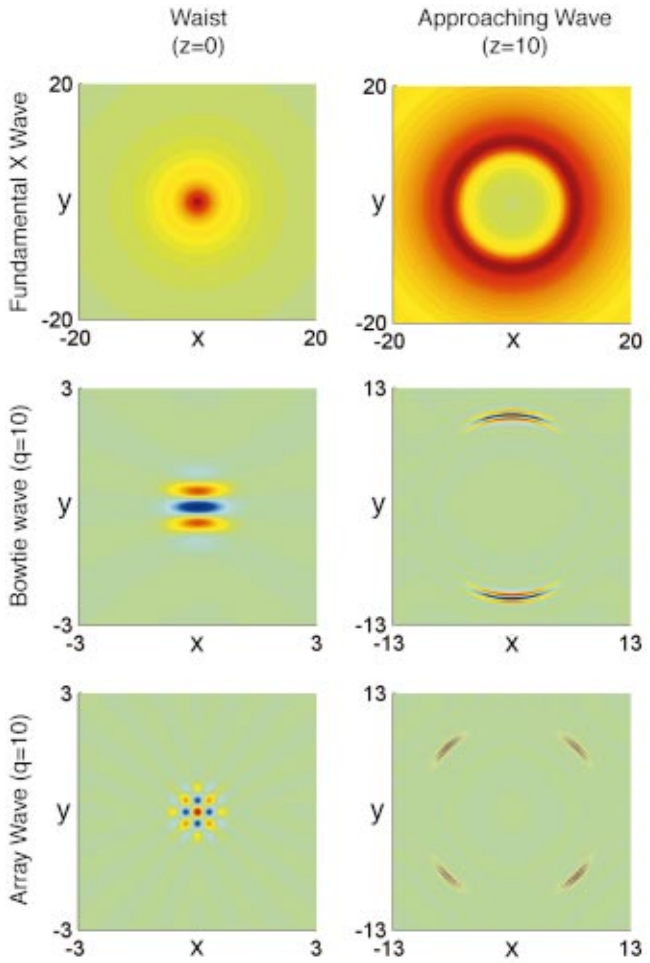

FIG. 6. (Color) Fundamental *X* wave, bowtie wave ($q=10$), and array wave ($q=10$). The rotationally invariant *X* wave $\Phi_{0,0}$ has a circular waist and an annular approaching form (cf. Fig. 1 for the geometry). For the bowtie waves, the energy essentially propagates along the *y* axis making the wave narrower in the *x* direction. The array wave is formed from wave components propagating along $y=\pm x$ leading to a grid-shaped waist for the wave. Each wave has been individually scaled. The increasing localization of the bowtie and array waves, in comparison to the fundamental *X* wave, is due to their higher spectral order. Note that each derivative increases the spectral order by one; thus, the spectral order of a $q=10$ bowtie wave is 10 while that of the array wave is 20.

Although mixed-wave modes naturally appear for derivatives of nondiffracting waves, they are usually studied for more practical reasons. For single-mode waves, the energy flow is effectively radially symmetric and the transducer arrangement, optical or acoustic, needs to be circular. Thus, the central pulse requires a large free medium for undistorted propagation. Mixed-wave modes, especially the bowtie waves, may be used to reduce the spatial volume needed for the wave propagation.

D. Extended nondiffracting waves

There are essentially two kinds of extended nondiffracting waves: (i) The Neumann solutions that are radial standing-wave solutions, thus resembling the Bessel solutions, but

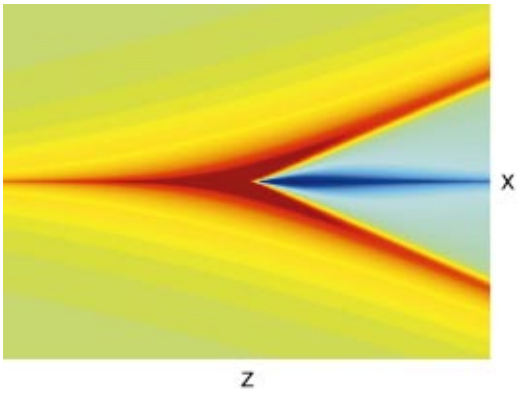

FIG. 7. (Color) Fundamental Y wave $\Phi_{0,0}^{H^{(2)}}$. The cross section of this wave resembles the capital letter Y since it contains only one half of the cone of propagation, and a divergence on the axis.

with a divergence on the axis of propagation and (ii) the Hankel solutions that describe an energy flux with a radial component. The energy may be carried either away from the axis of propagation (first Hankel wave) or towards the axis (second Hankel wave). Correspondingly, the Hankel waves assume an energy source on the axis of propagation and thus they do not satisfy the free-space wave equation on the axis.

The energy propagation is most conveniently analyzed in the far-field regime from the axis of propagation. Using an asymptotic expansion for the Hankel functions we find that the wave away from the z axis (for large r) is given by

$$\Phi_{H_n}^{(1,2)}(r,\varphi,z,t;\omega)=\frac{\sqrt{2}e^{in\varphi}(-1)^{*n}}{\sqrt{\pi\omega r\sin\zeta/c}}e^{\pm i[\omega r(\sin\zeta)/c-n\pi/2-\pi/4]}\times e^{i[(\cos\zeta)z/c-t]\omega}. \tag{44}$$

Therefore, the first Hankel wave $\Phi_{H_n}^{(1)}$ carries energy away from the axis of propagation. Hence, we call it a ''source field,'' while the second Hankel wave $\Phi_{H_n}^{(2)}$ transports energy in the opposite direction, which justifies the name ''sink field.'' In analogy with the motivation for the name ''X wave,'' we wish to introduce the term ''Y wave'' for the second Hankel wave $\Phi_{H_n}^{(2)}$ whose cross section in the (x,z) plane resembles the letter Y (see Fig. 7). Figure 8 illustrates the fundamental X wave, and the corresponding Neumann X wave and the two Hankel Y waves. In addition to their radial energy flux, the Hankel waves of higher azimuthal orders also feature an azimuthal energy flux that makes them rotational wave solutions. Due to the rotational shape of the higher azimuthal orders, these fields are also called spiral waves [13].

Although the singular behavior of the extended wave solutions emphasizes their mathematical nature, we argue that they are conceptually useful. Neumann-type solutions arise, for instance, in fluid dynamics when a bar is placed on the axis of propagation. If the bar is rigid enough to reflect all waves supported by the fluid, the field described by the scalar wave equation should vanish on the surface of the bar. This can in general be satisfied by taking an appropriate linear combination of Bessel- and Neumann-type solutions (with real coefficients). This leads to a nondiffracting wave

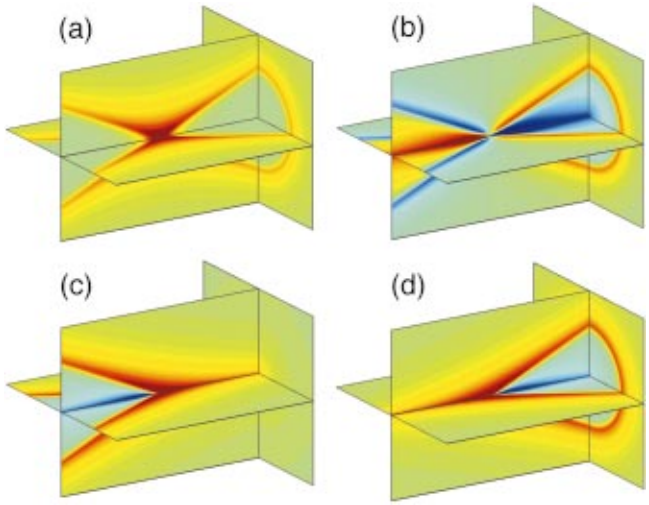

FIG. 8. (Color) (a) Fundamental X wave $\Phi_{0,0}$, (b) extended Neumann X wave $\Phi_{0,0}^{Y}$, (c) extended Hankel wave $\Phi_{0,0}^{H^{(1)}}$ (inverted Y wave), and (d) extended Hankel wave $\Phi_{0,0}^{H^{(2)}}$ (fundamental Y wave). The Neumann wave diverges along the axis of propagation and, especially, in the focal center of the wave. The ordinary Bessel-based wave and the extended Neumann wave contain both parts of the cone of propagation owing to the fact that both waves correspond to monochromatic standing-wave solutions. The Hankel wave $\Phi_{0,0}^{H^{(1)}}$ in (c) contains only the outward propagating half-cone that diverges in the focal center. Similarly, the Hankel wave $\Phi_{0,0}^{H^{(2)}}$ in (d) only contains the inward propagating half-cone.

without the central peak. On the other hand, only the zero Bessel order nondiffracting wave has the central peak while the other Bessel orders produce ''dark pulses'' [7] whose field amplitude vanishes on the beam or pulse center.

The Hankel-type solutions arise in physical experiments where the wave is generated by a planar or a conical aperture. For further discussion on Hankel waves, see Refs. [13,14]. Only the second Hankel wave needs to be emitted since it carries energy towards the axis of propagation. Since no physical sink exists on the axis, the energy is later on carried away from it. This ''generates'' the outward propagating component of the ordinary Bessel beam and cancels the singularity of a true Hankel wave. Note that the resultant wave is no longer a nondiffracting wave since the Hankel wave transforms into a Bessel wave. The central beam, however, remains unchanged and can thus be considered nondiffracting.

VIII. DISCUSSION

We have suggested a simple unified approach to nondiffracting waves using the Fourier representation for uniformly propagating solutions of the wave equation. This naturally leads to the spectral generalization of Bessel beams. While Bessel beams are monochromatic nondiffracting waves, their spectral Fourier transforms are waves that correspond to a unit impulse in the time domain. Thus, we obtain both a spectral and a temporal representation for nondiffracting waves.

We have also explicitly studied a specific subclass of broadband nondiffracting waves referred to as X waves. Their spectrum is limited to a given functional form (poly-

nomial in $\omega)\times e^{-\alpha\omega}$. This set of nondiffracting waves can be expressed algebraically, and it has been shown to be closed with respect to all spatial and temporal derivatives. This facilitates the description of new nondiffracting wave solutions using, for instance, bowtie and array wave techniques. We have also considered extended nondiffracting waves based on the Neumann or Hankel—instead of Bessel—functions, leading to the new class of *Y* waves. They offer a practical tool for the analysis and design of nondiffracting wave fields and the construction of appropriate antenna structures to be applied in the actual physical generation of limited-diffraction waves.

Finally, we have discussed and demonstrated several nondiffracting wave solutions and their physical properties. While rigorously nondiffracting waves only exist as purely mathematical entities, they can be approximately realized to obtain useful wave modes with large depth of field. We have discussed such properties of the wave solutions that are relevant for the design of the appropriate nondiffracting waves.

An increasing number of novel and important applications has been suggested for nondiffracting or limited-diffraction waves, ranging from optical microlithography [32] to particle acceleration [52]. Nondiffracting waves have also been applied in medical real-time imaging [33] while new potential can be foreseen within optical guidance and ranging techniques [28]. The present paper aims at simplifying the mathematical description of nondiffracting waves both within acoustics and optics.

ACKNOWLEDGMENTS

One of us (J.S.) acknowledges Helsinki University of Technology and the Finnish Cultural Foundation for financial support. We thank the Center for Scientific Computing (CSC, Espoo, Finland) for resources. This research was supported by the Academy of Finland through the Programme for Electronics Materials and Microsystems (EMMA). We also thank Professor Antti Räisänen (Radio Laboratory, Helsinki University of Technology) for inspiring discussions on microwave applications.

APPENDIX: ALGEBRAIC REPRESENTATION OF *X* WAVES

Since the argument $Q=\tau/\sqrt{\tau^2+b^2}$ in Eq. (20) satisfies $|Q|\leqslant 1$, we may express the Legendre functions in terms of generalized hyperbolic functions as [cf. Ref. [20], Eq. 8.704]

$$P_\nu^\mu(Q)=\frac{1}{\Gamma(1-\mu)}\left(\frac{1+Q}{1-Q}\right)^{\mu/2}\times {}_2F_1\left(-\nu,\nu+1;1-\mu;\frac{1-Q}{2}\right), \tag{A1}$$

whence

$$P_m^{-|n|}(Q)=\frac{1}{|n|!}\left(\frac{1-Q}{1+Q}\right)^{|n|/2}\times {}_2F_1\left(-m,m+1;|n|+1;\frac{1-Q}{2}\right). \tag{A2}$$

From here on we omit the absolute value signs from $|n|$ for convenience, but they must be inserted if negative n's are considered. Since either of the first two parameters in ${}_2F_1$ is a negative integer, the series expression for the hypergeometric function is finite, and it is therefore only a polynomial in $(1-Q)$. The hypergeometric function is defined as

$${}_2F_1(a_1,a_2;b;z)=\sum_{k_0}^{\infty}\frac{(a_1)_k(a_2)_k}{(b)_k}\frac{z^k}{k!}, \tag{A3}$$

where $(q)_k$ is the Pochhammer symbol defined as

$$(q)_0=1,$$

$$(q)_k=q(q+1)(q+2)\cdots(q+k-1)=\frac{(q+k-1)!}{(q-1)!}. \tag{A4}$$

The above expression [Eq. (A3)] is valid as long as the factorials are well defined. Hence,

$$\begin{aligned}{}_2F_1(-m,m+1;n+1;z)&=\sum_{k=0}^{\infty}\frac{(-m)(-m+1)\ldots(-m+k-1)(m+1)(m+2)\ldots(m+k)}{(n+1)(n+2)\cdots(n+k)}\frac{z^k}{k!}\\&=\sum_{k=0}^{\infty}(-1)^k\frac{(m)(m-1)\cdots(m-k+1)(m+1)(m+2)\cdots(m+k)}{(n+1)(n+2)\cdots(n+k)}\frac{z^k}{k!}.\end{aligned} \tag{A5}$$

The sum terminates once the numerator vanishes, which limits the summation into the range $k\leqslant m$. Therefore, the hypergeometric function may be expressed as

$${}_2F_1(-m,m+1;n+1;z)=\sum_{k=0}^{m}(-1)^k\frac{(m+k)!/(m-k)!}{(n+k)!/n!}\frac{z^k}{k!}. \tag{A6}$$

If we further choose the variable $M=\tau^2+b^2$ the wave solutions, Eq. (20), can be expressed as

$$\Phi_{n,m}=(-1)^{*n}e^{in\varphi}\frac{\Gamma(m+|n|+1)}{(\sqrt{M})^{m+1}}\left(\frac{1-Q}{1+Q}\right)^{|n|/2}\times\sum_{k=0}^{m}(-1)^k\frac{(m+k)!/(m-k)!}{(|n|+k)!}\frac{(1-Q)^k}{2^k k!}. \tag{A7}$$

This expression simplifies greatly for some special cases. If

in the summation we write $(1-Q)/2=1-(1+Q)/2$, and use the binomial theorem, the sum is

$$\sum_{k=0}^{m}(-1)^k\frac{(m+k)!/(m-k)!}{(|n|+k)!}\frac{(1-Q)^k}{2^k k!}$$
$$=\sum_{j=0}^{m}(-1)^j\left[\sum_{k=j}^{m}(-1)^k\frac{(m+k)!/(m-k)!}{(|n|+k)!k!}\times\frac{k!}{j!(k-j!)}\right]\left(\frac{1+Q}{2}\right)^j. \tag{A8}$$

By setting $k'=k-j$ and $M=m-j$, the coefficients are found to equal

$$\frac{(-1)^j}{j!}\sum_{k'=0}^{M}(-1)^{k'}\frac{(m+k'+j)!/(M-k')!}{(|n|+k'+j)!k'!}. \tag{A9}$$

If now $m=|n|$ and $j\neq m$, the above expression vanishes since

$$\frac{(-1)^j}{j!M!}\sum_{k'=0}^{M}\frac{M!}{(M-k')!k'!}(-1)^{k'}=\frac{(-1)^j}{j!M!}(1-1)^M=0. \tag{A10}$$

For $j=m$, i.e., $M=0$, the coefficient is simply $(-1)^m/m!$. Hence, for $m=|n|$ we have

$$\sum_{k=0}^{m}(-1)^k\frac{(m+k)!/(m-k)!}{(|n|+k)!}\frac{(1-Q)^k}{2^k k!}=\frac{1}{m!}\left(\frac{1+Q}{2}\right)^m, \tag{A11}$$

and the wave may be represented as

$$\Phi_{|n|,n}=(-1)^{*n}e^{in\varphi}\frac{\Gamma(2|n|+1)}{(\sqrt{M})^{|n|+1}}\left(\frac{1-Q}{1+Q}\right)^{|n|/2}\frac{1}{|n|!}\left(\frac{1+Q}{2}\right)^{|n|}$$
$$=(-1)^{*n}e^{in\varphi}\frac{(2|n|)!}{|n|!2^{|n|}}\frac{b^{|n|}}{(\tau^2+b^2)^{|n|+1/2}}. \tag{A12}$$

On the other hand, for $m=0$, we obtain from Eq. (A7)

$$\Phi_{n,0}=(-1)^{*n}e^{in\varphi}\frac{1}{\sqrt{M}}\left(\frac{1-Q}{1+Q}\right)^{|n|/2}$$
$$=(-1)^{*n}e^{in\varphi}\frac{1}{\sqrt{\tau^2+b^2}}\frac{b^{|n|}}{(\sqrt{\tau^2+b^2}+\tau)^{|n|}}. \tag{A13}$$

Finally, for $m=n=0$ this expression reduces to

$$\Phi_{0,0}=\frac{1}{\sqrt{\tau^2+b^2}}, \tag{A14}$$

for the fundamental X wave.

[1] J. Durnin, J. J. Miceli, Jr., and J. H. Eberly, Phys. Rev. Lett. **58**, 1499 (1987).

[2] J. A. Stratton, *Electromagnetic Theory* (McGraw-Hill, New York, 1941).

[3] J. Lu and J. F. Greenleaf, IEEE Trans. Ultrason. Ferroelectr. Freq. Control **37**, 438 (1990).

[4] J. Lu and J. F. Greenleaf, IEEE Trans. Ultrason. Ferroelectr. Freq. Control **39**, 19 (1992).

[5] J. Lu, X.-L. Xu, and J. F. Greenleaf, IEEE Trans. Ultrason. Ferroelectr. Freq. Control **42**, 850 (1995).

[6] J. Fagerholm *et al.*, Phys. Rev. E **54**, 4347 (1996).

[7] A. T. Friberg, J. Fagerholm, and M. M. Salomaa, Opt. Commun. **136**, 207 (1997).

[8] P. R. Stepanishen and J. Sun, J. Acoust. Soc. Am. **102**, 3308 (1997).

[9] P. R. Stepanishen, J. Acoust. Soc. Am. **103**, 1742 (1998).

[10] J. Salo, F. Fagerholm, A. T. Friberg, and M. M. Salomaa, Phys. Rev. Lett. **83**, 1171 (1999).

[11] J. Lu, IEEE Trans. Ultrason. Ferroelectr. Freq. Control **42**, 1050 (1995).

[12] J. Lu, Int. J. Imaging Syst. Technol. **8**, 127 (1997).

[13] S. Chávez-Cerda, G. S. McDonald, and G. H. C. New, Opt. Commun. **123**, 225 (1996).

[14] S. Chávez-Cerda, J. Mod. Opt. **46**, 923 (1999).

[15] We choose to define the *n*-dimensional direct and inverse Fourier transforms symmetrically, i.e., both have the constant coefficient $(2\pi)^{-n/2}$.

[16] M. S. Patterson and F. S. Foster, IEEE Trans. Sonics Ultrason. **SU-29**, 83 (1982).

[17] If the value of ζ is not fixed, we can integrate over $\zeta\in[0,\pi]$ and, therefore, all free space solutions of the scalar wave equation can be decomposed into nondiffracting waves with different ζ's, i.e., with different velocities.

[18] R. Donnelly, D. Power, G. Templemen, and A. Whalen, IEEE Trans. Ultrason. Ferroelectr. Freq. Control **41**, 7 (1994).

[19] Note that $f_n(\omega)$ is not the true spectrum of the wave since the Fourier representation of the nondiffracting wave contains the $1/k_\perp\propto 1/\omega$ term whence the frequency spectrum is actually proportional to $f_n(\omega)/\omega$.

[20] I. S. Gradshteyn and I. M. Ryzhik, *Table of Integrals, Series, and Products* (Academic Press, New York, 1965).

[21] Actually, a ''sink'' or a ''source'' cannot be defined mathematically, we must merely exclude the *z* axis from the space.

[22] M. Abramowitz and I. Stegun, *Handbook of Mathematical Functions* (Dover, New York, 1965).

[23] Donnelly *et al.* (Ref. [18]) used the Fourier method to derive the X wave $\Phi_{0,1}$.

[24] The angular spectrum representation of nondiffracting waves may also be extended to include evanescent Bessel waves and their spectral generalizations. These waves are not, however, nondiffracting since their field amplitudes decay exponentially under propagation [53].

[25] R. Piestun and J. Shamir, J. Opt. Soc. Am. A **15**, 3039 (1998).

[26] T. Koike, K. Yamada, and K. Nakamura, Jpn. J. Appl. Phys., Part 1 **34**, 2610 (1995); **35**, 3184 (1996); Electron. Lett. **32**, 2304 (1996).

[27] D. K. Hsu, F. J. Margetan, and D. O. Thompson, Appl. Phys. Lett. **55**, 2066 (1989).

[28] L. C. Laycock and S. C. Webster, GEC J. Res. **10**, 36 (1992).
[29] J. Turunen, A. Vasara, and A. T. Friberg, Appl. Opt. **27**, 3959 (1988).
[30] G. Indebetouw, J. Opt. Soc. Am. A **6**, 150 (1988).
[31] P. Saari and H. S̃onajalg, Laser Phys. **7**, 32 (1997).
[32] M. Erdélyi *et al.*, J. Vac. Sci. Technol. B **15**, 287 (1997).
[33] J. Lu, T. K. Song, R. R. Kinnick, and J. F. Greenleaf, IEEE Trans. Med. Imaging **12**, 819 (1993).
[34] J. Lu and J. F. Greenleaf, IEEE Trans. Ultrason. Ferroelectr. Freq. Control **41**, 724 (1994).
[35] J. Lu, IEEE Trans. Ultrason. Ferroelectr. Freq. Control **44**, 181 (1997).
[36] C. Paterson and R. Smith, Opt. Commun. **124**, 121 (1996).
[37] E. M. Frins, J. A. Ferrari, A. Dubra, and D. Perciante, Opt. Lett. **25**, 284 (2000).
[38] C. Paterson and R. Smith, Opt. Commun. **124**, 131 (1996).
[39] J. Arlt and K. Dholakia, Opt. Commun. **177**, 297 (2000).
[40] T. Hirvonen, J. P. S. Ala-Laurinaho, J. Tuovinen, and A. V. Räisänen, IEEE Trans. Antennas Propag. **45**, 1270 (1997); Microwave Opt. Technol. Lett. **15**, 134 (1997).
[41] N. Guérineau and J. Primot, J. Opt. Soc. Am. **16**, 293 (1999).
[42] C. Yu, M. R. Wang, A. J. Varela, and B. Chen, Opt. Commun. **177**, 369 (2000).
[43] J. Lu and J. F. Greenleaf, IEEE Trans. Ultrason. Ferroelectr. Freq. Control **39**, 441 (1992).
[44] S. Ballandras *et al.*, in *IEEE Ultrasonics Symposium Proceedings* (IEEE, New York, 1999), pp. 1159–1162.
[45] J. Lu, IEEE Trans. Ultrason. Ferroelectr. Freq. Control **43**, 893 (1996).
[46] T. Sehm, A. Lehto, and A. V. Räisänen, IEEE Trans. Antennas Propag. **47**, 1125 (1999).
[47] P. Saari and K. Reivelt, Phys. Rev. Lett. **79**, 4135 (1997).
[48] J. Lu and S. He, Opt. Commun. **161**, 187 (1999).
[49] The cross section L_2 norm of the fundamental mode is infinite since the mode decays as $1/r$. Therefore $\int|\Phi_{00}(z=t=0)|^2 dxdy=\infty$ and although the wave appears localized, it in fact is not.
[50] See, for example, Ref. [12] where the grid and layered array beams have $|c_n|=1$ for all n. In particular, the grid array beam has $c_n=i^n e^{in}$ [54], whence the wave is no longer localized but retains a constant, periodic form for $r\rightarrow\infty$.
[51] J. Lu and J. F. Greenleaf, IEEE Trans. Ultrason. Ferroelectr. Freq. Control **40**, 735 (1993).
[52] B. Hafizi *et al.*, Phys. Rev. E **60**, 4779 (1999).
[53] S. Ruschin and A. Leizer, J. Opt. Soc. Am. A **15**, 1139 (1998).
[54] J. Lu, in *IEEE Ultrasonics Symposium Proceedings* (IEEE, New York, 1996), pp. 1255–1260.
[55] S. Chávez-Cerda, M. A. Meneses-Nava, and J. M. Hickmann, Opt. Lett. **23**, 1871 (1998).